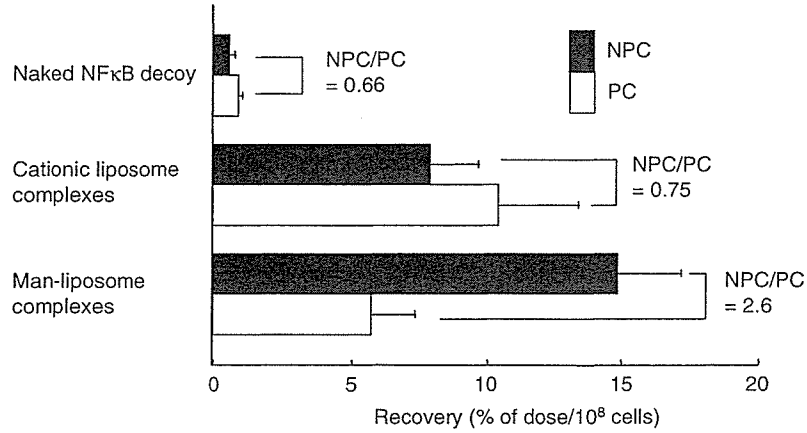

Fig. 2. Intrahepatic distribution of ^{32}P-labeled naked NFκB decoy, cationic liposome/^{32}P-labeled NFκB decoy complex and Man-liposome/^{32}P-labeled NFκB decoy complex after intravenous injection into mice. ^{32}P-labeled NFκB was complexed with mannosylated liposomes or cationic liposomes at a charge ratio of 2.3:1.0 (+:−). Radioactivity was determined in NPC (■) and PC (□). Each value represents the mean ± S.D. (n = 3).

noassay (EIA) to confirm directly the inhibitory effect of Man-liposome/NFκB decoy complex on the activation of NFκB. After LPS treatment, the amount of activated NFκB was dramatically increased. However, after injection of Man-liposome/NFκB decoy complex, the amount of activated NFκB in nuclei did not increase with LPS treatment (Fig. 6).

4. Discussion

Recently, new techniques to inhibit target gene expression using oligonucleotides, such as decoy oligonucleotides, antisense DNA, ribozyme and siRNA, have been developed, which are expected to be attractive treatments without side-effects on genome DNA compared with pDNA. However, oligonucleotides are easily degraded in blood and rapidly metabolized and, therefore, potential carriers have to be developed capable of carrying enough oligonucleotide to produce a therapeutic effect. As far as NFκB decoy therapy for endotoxin syndrome is concerned, since Kupffer cells play an important role of producing cytokines, NFκB decoy taken up by Kupffer cells could effectively inhibit NFκB-mediated inflammatory cytokine production. In this respect, in order to achieve a therapeutic effect with NFκB decoy, it is necessary to develop a Kupffer cell-targeting carrier for NFκB decoy. Previously, we have developed a novel pDNA carrier system for NPC targeting involving Man-liposomes, which could effectively achieve cell-specific transfer to NPC and macrophages in vivo and in vitro [20–22]. Man-liposomes are an attractive tool for NFκB decoy delivery to Kupffer cells, although the physicochemical properties, such as molecular weight and size, of the NFκB decoy and pDNA are very different. Therefore, the purpose of this study was to investigate the distribution and therapeutic effect of Man-liposome/NFκB decoy complex on endotoxin syndrome.

To investigate NPC selective delivery of NFκB decoy by Man-liposomes, the tissue and intrahepatic distribution of Man-liposome/[^{32}P] NFκB decoy complex were examined. In this study, Man-liposome/[^{32}P] NFκB decoy complex exhibited rapid and high accumulation in the liver (Fig. 1). This result was well concerned with the tissue accumulation of Man-liposome/pDNA complex after intravenous injection [22]. As far as intrahepatic distribution is concerned, the Man-liposome/NFκB decoy complex was preferentially taken up by NPC (Fig. 2). This result also agreed with the intrahepatic distribution of Man-liposome/pDNA complex [22]. Considering that mannose receptors are expressed on NPC [17], these results are in good agreement with the intrahepatic distribution of Man-liposome/NFκB decoy complex (Fig. 2). Moreover, Gal-liposome/NFκB decoy complex could not inhibit cytokine production, comparing to the same amount of NFκB decoy delivered by Man-liposome showed significantly inhibitory effect (Fig. 3B). Gal-liposome/NFκB decoy complex would be preferentially taken up by hepatocyte not by NPC, since a large number of asiaroglycoprotein receptor, which could recognize galactose, was expressed on hepatocyte not NPC [28]. These results supported the mannose receptor-mediated uptake of Man-liposome/NFκB decoy complex.

To determine the therapeutic effect of Man-liposome/NFκB decoy complex, we investigated the inhibitory effect on cytokine production and liver injury measuring serum ALT and AST. The inhibitory effect of Man-liposome/NFκB decoy complex on cytokine production was determined by measuring the serum concentration of LPS-induced TNFα, which induced other kinds of cytokine production and inflammation (Fig. 4). Man-liposome/NFκB decoy complex significantly inhibited the production of these cytokines compared with the same dose of naked NFκB decoy and bare cationic liposome/NFκB decoy. Increase of serum ALT and AST, which indicate hepatocytes injury caused by inflammatory cytokines, were also prevented by Man-liposome/NFκB decoy complex but not by naked NFκB decoy. These results suggest that NFκB decoy is effectively delivered to Kupffer cells by Man-liposomes. This result agrees with the intrahepatic distribution of Man-liposome/NFκB decoy complex after intravenous injection (Fig. 2).

In order to evaluate whether Man-liposome/NFκB decoy complex could inhibit NFκB-mediated transcription, the amount of activated NFκB in the nuclei was determined by EIA (Fig. 6). The amount of activated NFκB in the liver nuclei was reduced by Man-liposome/NFκB decoy complex, which

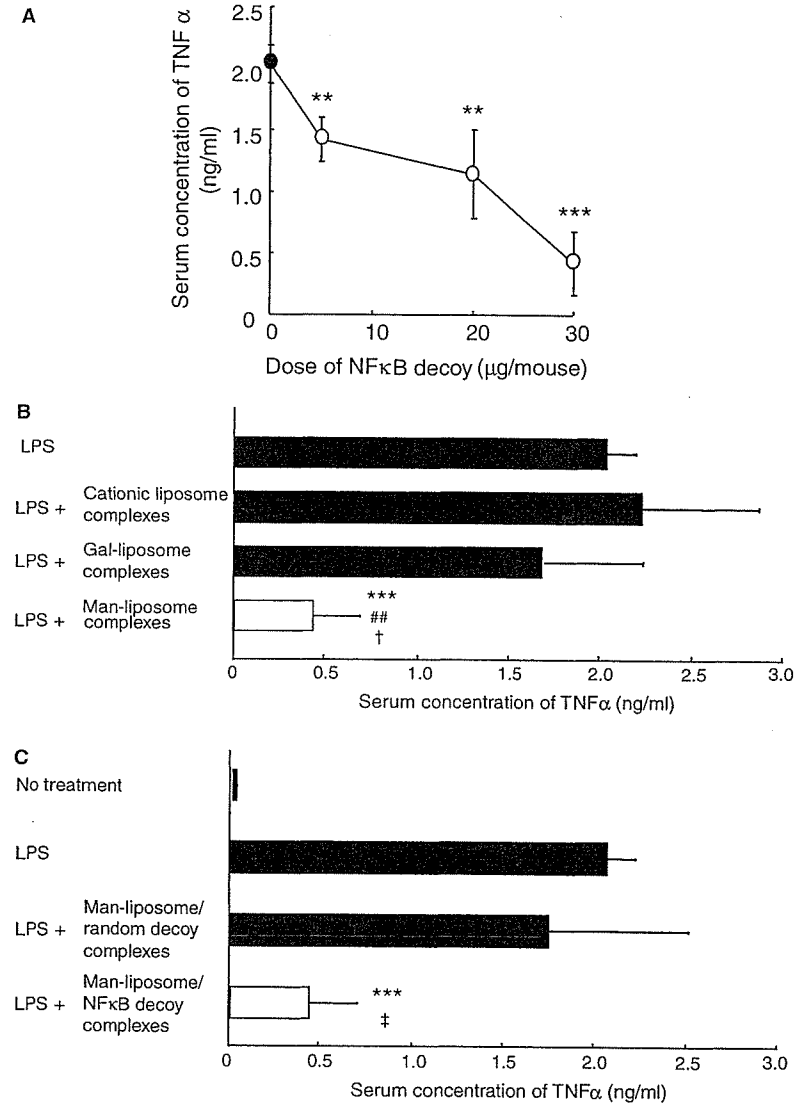

Fig. 3. Inhibitory effect of Man-liposome/NFκB decoy complex on the production of TNFα at different doses (A), several kinds of liposomes/NFκB decoy complexes (B) and the sequence of the decoy (C). Serum concentration of TNFα was determined by ELISA. One minute after intravenous administration of LPS, Man-liposome/NFκB decoy complex or Man-liposome/random decoy complex was intravenously injected into mice. Blood was collected from the vena cava at 1 h. Each value represents the mean ± S.D. ($n = 3, 4$). Significant difference: $^{***}P < 0.001$ vs. (LPS); $^{\#\#}P < 0.01$ vs. (LPS + cationic liposome complexes); $^{\dagger}P < 0.05$ vs. (LPS + Gal-liposome complexes); $^{\ddagger}P < 0.05$ vs. (LPS + Man-liposome/random decoy complex).

suggests that NFκB decoy binds to NFκB and inhibits translocation of NFκB into the nuclei. In addition, the production of IFNγ and IL-1β was also inhibited by the Man-liposome/NFκB decoy complex (Fig. 4), however, TNFα production could not be inhibited by the Man-liposome/random decoy complex. This result suggests that the sequence of the NFκB decoy is important for the inhibition of NFκB activation. These results confirm that NFκB decoy delivered by Man-liposomes is able to inhibit NFκB-mediated transcription. Since NFκB decoy can inhibit several kinds of NFκB-mediated cytokine production at the same time, cell-specific delivery of NFκB decoy will contribute to the novel therapy of other diseases involving several kinds of inflammatory cytokines.

As far as the therapy of liver disease evoked cytokine production by Kupffer cells is concerned, a Kupffer cell-targeting carrier is required for the effective therapy with NFκB decoy. To date, some carriers, including HVJ liposomes [14] and bare cationic liposomes [13], have been used as NFκB carriers to inhibit Kupffer cell cytokine production. However, because these carriers deliver NFκB decoy to any liver cells, the amount of NFκB decoy delivered to Kupffer cells is small considering that the number of Kupffer cells account for only 15% of the total number of liver cells [17]. In our previous study of bare cationic liposomes, after intravenous injection, bare cationic liposome/NFκB decoy complex gradually accumulated in the liver after rapid accumulation in the lung [13]. This rapid accumulation in the lung agreed with the distribution of cationic liposomes [29] and cationic liposome/pDNA complex [22,30]. As far as the intrahepatic distribution of bare cationic liposome/NFκB decoy is concerned, NPC/PC of cationic liposome/NFκB decoy was 1/3-fold lower than that of Man-liposome/NFκB decoy complex (Fig. 2). Considering

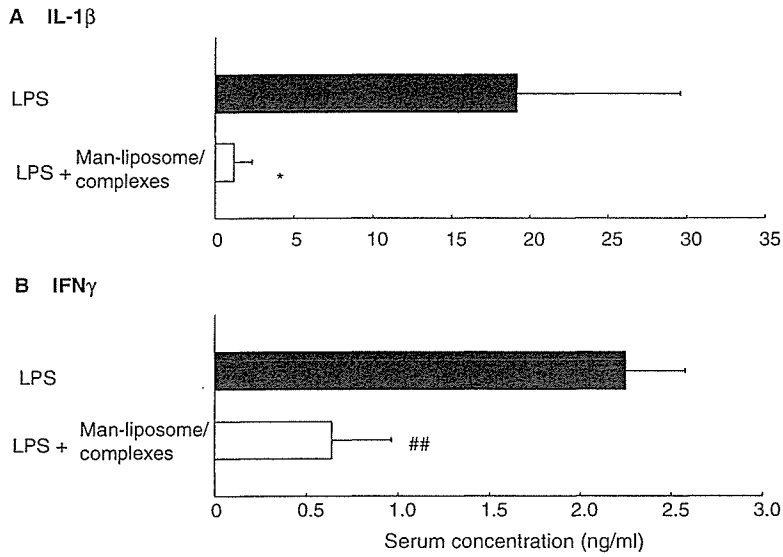

Fig. 4. Inhibitory effect of Man-liposome/NFκB decoy complex or Man-liposome/random decoy complex on the production of IL-1β (A) and IFNγ (B). One minute after intravenous administration of LPS, Man-liposome/NFκB decoy complex (30 μg/mouse) was intravenously injected into mice. Blood was collected from the vena cava at 3 h (IL-1β) and 6 h (IFNγ). Each value represents the mean ± S.D. ($n = 3$). Significant difference: $^{*}P < 0.05$ vs. (LPS in A); $^{\#\#}P < 0.01$ vs. (LPS in B).

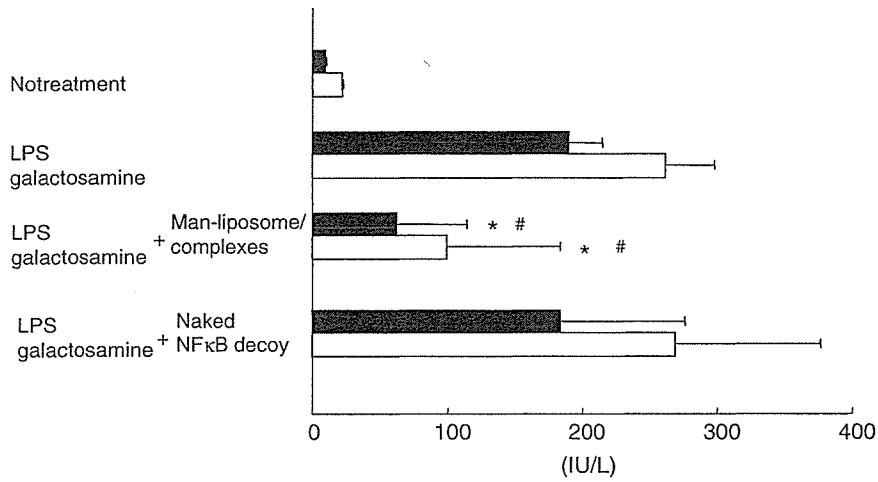

Fig. 5. Inhibitory effect of Man-liposome/NFκB decoy complexes on liver injury. One minute after intraperitoneal administration of LPS and D-(+)-galactosamine, Man-liposome/NFκB decoy complex (30 μg/mouse) or naked NFκB decoy were intravenously injected into mice. Blood was collected from the vena cava at 6 h. Serum concentration was determined in ALT (■) and AST (□). Each value represents the mean ± S.D. ($n \geqq 4$). Significant difference: $^{*}P < 0.05$ vs. (LPS); $^{\#}P < 0.05$ vs. (LPS + naked NFκB decoy).

the liver accumulation, these results suggested that the amount of NFκB decoy delivered by bare cationic liposomes is much lower than that by Man-liposomes. The results of this distribution study are in agreement with the pharmacological results showing that bare cationic liposome/NFκB decoy complex cannot suppress cytokine production while the same amount of NFκB decoy complexed with Man-liposomes significantly inhibits cytokine production (Fig. 3B). These results provide evidence that Kupffer cell-selective delivery is important for prevention of cytokines production.

In the present study, we demonstrated that Kupffer cell-selective delivery using Man-liposomes effectively inhibits cytokine production by Kupffer cells and liver injury caused by cytokines. Recently, we demonstrated that fucose-decorated bovine serum albumin, as a model macromolecular compound, was preferentially taken up by Kupffer cells via recognition by fucose receptors, which are uniquely expressed on Kupffer cells [31,32]. Therefore, fucose decoration of cationic liposomes may improve Kupffer cell-targeting delivery for NFκB decoy therapy. Based on the results of this study, we now intend to investigate fucosylated cationic liposomes.

In conclusion, Man-liposome/NFκB decoy complex showed specific accumulation in NPC and markedly suppressed the effect of NFκB-mediated inflammatory cytokine production and liver injury after intravenous injection. It was shown that NFκB decoy was delivered by Man-liposomes via mannose

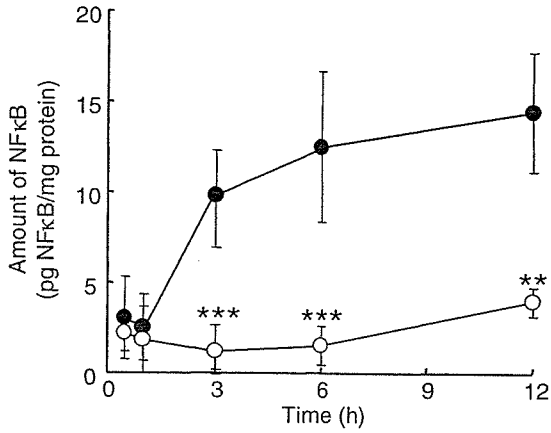

Fig. 6. Inhibitory effect of Man-liposome/NFκB decoy complex on NFκB activation in the nuclei. One minute after intravenous administration of LPS, Man-liposome/NFκB decoy complex (30 μg/mouse) (○) or 5% dextrose (●) was intravenously injected into mice. Liver was excised at 0.5, 1, 3, 6, 12 h and nuclear protein was extracted. Each value represents the mean ± S.D. ($n = 3$). Significant difference: $^{***}P < 0.001$, $^{**}P < 0.01$.

receptor recognition uptake. Following cell-specific delivery of NFκB decoy by Man-liposomes, NFκB in the nuclei in liver cells was attenuated and TNFα, IL1β and IFNγ production were inhibited at the same time. These observation lead us to believe that Man-liposomes are able to contribute to the development of new forms of therapy using oligonucleotides, such as antisense DNA, siRNA and so on.

Acknowledgements: This work was supported in part by Grant-in-Aids for Scientific Research from Ministry of Education, Culture, Sports, Science, and Technology of Japan, by Health and Labor Sciences Research Grants for Research on Advanced Medical Technology from the Ministry of Health, Labor and Welfare of Japan and by Radioisotope Research Center of Kyoto University.

References

[1] Roland, N., Wade, J., Davalos, M., Wendon, J., Philpott-Howars, J. and Williams, R. (2000) The system inflammatory response syndrome in acute liver failure. Hepatology 32, 734–739.
[2] Morrison, D.C. and Ryan, J.L. (1987) Endotoxins and disease mechanisms. Annu. Rev. Med. 38, 417–432.
[3] Iimuro, Y., Yamamoto, M., Kohno, H., Itakura, J., Fujii, H. and Matsumoto, Y. (1994) Blockade of liver macrophages by gadolinium chloride reduces lethality in endotoxemic rats analysis of mechanisms of lethality in endotoxemia. J. Leukoc. Biol. 55, 723–728.
[4] Arai, M., Mochida, S., Ohno, A., Ogata, I. and Fujiwara, K. (1993) Sinusoidal endothelial cell damage by activated macrophages in rat liver necrosis. Gastroenterology 104, 1466–1471.
[5] Pahl, H.L. (1999) Activations and target genes of Rel/NF-κB transcription factors. Oncogene 18, 6853–6866.
[6] Baeuerle, P.A. and Henkel, T. (1994) Function and activation of NF-κB in the immune system. Annu. Rev. Immunol. 12, 141–179.
[7] Wrighton, C.J., Hofer-Warbinek, R., Moll, T., Eytner, R., Bach, F.H. and de Martin, R. (1996) Inhibition of endothelial cell activation by adenovirus-mediated expression of IκBα, an inhibitor of the transcription factor NF-κB. J. Exp. Med. 183, 1013–1022.
[8] Foxwell, B., Browne, K., Bondeson, J., Clarke, C., de Martin, R., Brennan, F. and Feldmann, M. (1998) Efficient adenoviral infection with IκBα reveals that macrophage TNFα production in rheumatoid arthritis is NF-κB dependent. Proc. Natl. Acad. Sci. USA 95, 8211–8215.
[9] Bielinska, A., Shivdasani, R.A., Zhang, L.Q. and Nabel, G.J. (1990) Regulation of gene expression with double-stranded phosphorothioate oligonucleotides. Science 250, 997–1000.
[10] Morishita, R., Higaki, J., Tomita, N. and Ogihara, T. (1998) Application of transcription factor "decoy" strategy as means of gene therapy and study of gene expression in cardiovascular disease. Circ. Res. 82, 1023–1028.
[11] Morishita, R., Sugimoto, T., Aoki, M., Kida, I., Tomita, N., Moriguchi, A. and Maeda, K. (1997) In vivo transduction of cis element decoy against nuclear factor-κB binding site prevents myocardial infraction. Nat. Med. 3, 894–899.
[12] Morishita, R., Tomita, N., Kaneda, Y. and Ogihara, T. (2004) Molecular therapy to inhibit NFκB activation by transcription factor decoy oligonucleotide. Curr. Opin. Pharmacol. 4, 139–146.
[13] Higuchi, Y., Kawakami, S., Oka, M., Yamashita, F. and Hashida, M. (2006) Suppression of TNFα production in LPS induced liver failure mice after intravenous injection of cationic liposome/NFκB decoy complex. Pharmazie 61, 144–147.
[14] Ogushi, I., Iimuro, Y., Seki, E., Son, G., Hirano, T., Hada, T., Tsutsui, H., Nakanishi, K., Morishita, R., Kaneda, Y. and Fujimoto, J. (2003) Nuclear factor κB decoy oligonucleotides prevent endotoxin-induced fatal liver failure in a murine model. Hepatology 38, 335–344.
[15] Hirano, T., Fujimoto, J., Ueki, T., Yamamoto, H., Iwasaki, T., Morisita, R., Sawa, Y., Kaneda, Y., Takahashi, H. and Okamoto, E. (1998) Persistent gene expression in rat liver in vivo by repetitive transfections using HVJ-liposome. Gene Ther. 5, 459–464.
[16] Yoshida, M., Yamamoto, N., Uehara, T., Terao, R., Nitta, R., Harada, N., Hatano, E., Iimuro, Y. and Yamaoka, Y. (2002) Kupffer cell targeting by intraportal injection of the HVJ cationic liposome. Eur. Surg. Res. 34, 251–259.
[17] Kuiper, J., Brouwer, A., Knook, D.L. and van Berkel, T.J.C. (1994) Kupffer and sinusoidal endothelial cells in: The Liver: Biology and Pathobiology (Arias, I.M., Boyer, J.L., Fausto, N., Jakoby, W.B., Schachter, D.A. and Shafritz, D.A., Eds.), 3rd ed, pp. 791–818, Raven Press, NY.
[18] Dzau, V.J., Mann, M.J., Morishita, R. and Kaneda, Y. (1996) Fusigenic viral liposome for gene therapy in cardiovascular diseases. Proc. Natl. Acad. Sci. USA 93, 11421–11425.
[19] Hashida, M., Kawakami, S. and Yamashita, F. (2005) Lipid carrier systems for targeted drug and gene delivery. Chem. Pharm. Bull. 53, 871–880.
[20] Kawakami, S., Sato, A., Nishikawa, M., Yamashita, F. and Hashida, M. (2000) Mannose receptor-mediated gene transfer into macrophages using novel mannosylated cationic liposomes. Gene Ther. 7, 292–299.
[21] Kawakami, S., Hattori, Y., Lu, Y., Higuchi, Y., Yamashita, F. and Hashida, M. (2004) Effect of cationic charge on receptor-mediated transfection using mannosylated cationic liposome/plasmid DNA complexes following the intravenous administration in mice. Pharmazie 59, 405–408.
[22] Yamada, M., Nishikawa, M., Kawakami, S., Hattori, Y., Nakano, T., Yamashita, F. and Hashida, M. (2004) Tissue and intrahepatic distribution and subcellular localization of a mannosylated lipoplex after intravenous administration in mice. J. Control. Release 98, 157–167.
[23] Hattori, Y., Kawakami, S., Suzuki, S., Yamashita, F. and Hashida, M. (2004) Enhancement of immune responses by DNA vaccination through targeted gene delivery using mannosylated cationic liposome formulations following intravenous administration in mice. Biochem. Biophys. Res. Commun. 317, 992–999.
[24] Kawakami, S., Wong, J., Sato, A., Hattori, Y., Yamashita, F. and Hashida, M. (2000) Biodistribution characteristics of mannosylated, fucosylated, and galactosylated liposomes in mice. Biochim. Biophys. Acta 1524, 258–265.
[25] Hattori, Y., Suzuki, S., Kawakami, S., Yamashita, F. and Hashida, M. (2005) The role of dioleoylphosphatidylethanolamine (DOPE) in targeted gene delivery with mannosylated cationic liposomes via intravenous route. J. Control. Release 108, 484–495.

[26] Kawakami, S., Fumoto, S., Nishikawa, M., Yamashita, F. and Hashida, M. (2000) In vivo gene delivery to the liver using novel galactosylated cationic liposomes. Pharm. Res. 17, 306–313.
[27] Fumoto, S., Nakadori, F., Kawakami, S., Nishikawa, M., Yamashita, F. and Hashida, M. (2003) Analysis of hepatic disposition of galactosylated cationic liposome/plasmid DNA complexes in perfused rat liver. Pharm. Res. 20, 1452–1459.
[28] Kuiper, J. (1994) The Liver: Biology and Pathobiology, third ed, Raven Press, NY, p. 791.
[29] Yeeprae, W., Kawakami, S., Suzuki, S., Yamashita, F. and Hashida, M. (2006) Physicochemical and pharmacokinetic characteristics of cationic liposomes. Pharmazie 61, 102–105.
[30] Kawakami, S., Ito, Y., Fumoto, S., Yamashita, F. and Hashida, M. (2005) Enhanced gene expression in lung by a stabilized lipoplex using sodium chloride for complex formation. J. Gene Med. 7, 1526–1533.
[31] Higuchi, Y., Nishikawa, M., Kawakami, S., Yamashita, F. and Hashida, M. (2004) Uptake characteristics of mannosylated and fucosylated bovine serum albumin in primary cultured rat sinusoidal endothelial cells and Kupffer cells. Int. J. Pharm. 287, 147–154.
[32] Opanasopit, P., Nishikawa, M., Yamashita, F., Takakura, Y. and Hashida, M. (2001) Pharmacokinetic analysis of lectin-dependent biodistribution of fucosylated bovine serum albumin: a possible carrier for Kupffer cells. J. Drug Target. 9, 341–351.

Available online at www.sciencedirect.com
SCIENCE DIRECT
Journal of Controlled Release 114 (2006) 69–77
journal of controlled release
www.elsevier.com/locate/jconrel

Biodistribution characteristics of amino acid dendrimers and their PEGylated derivatives after intravenous administration

Tatsuya Okuda [a,b], Shigeru Kawakami [a], Tadahiro Maeie [a], Takuro Niidome [c], Fumiyoshi Yamashita [a], Mitsuru Hashida [a,*]

[a] *Department of Drug Delivery Research, Graduate School of Pharmaceutical Sciences, Kyoto University, 46-29 Yoshida-Shimo-Adachi-cho, Sakyo-ku, Kyoto 606-8501, Japan*
[b] *Japan Association for the Advancement of Medical Equipment, 3-42-6 Hongo, Bunkyo-ku, Tokyo113-0033, Japan*
[c] *Department of Applied Chemistry, Faculty of Engineering, Kyushu University, 744 Motooka, Nishi-ku, Fukuoka 819-0395, Japan*

Received 14 March 2006; accepted 14 May 2006
Available online 23 May 2006

Abstract

In this study, we synthesized dendritic poly(L-lysine)s (DPKs), dendritic poly(L-ornithine)s (DPOs), which are constructed as novel amino acid dendrimers, and PEGylated KG6 (the sixth generation of DPKs), and evaluated the physicochemical properties and biodistribution characteristics of these dendrimers. The particle size of DPKs and DPOs was well controlled in the nanometer range. The zeta-potential of these dendrimers was slightly positive and this gradually increased in association with their generation. After intravenous administration to mice, all tested dendrimers cleared rapidly from blood flow and mainly accumulated in the liver and kidney. The hepatic and renal accumulation changed in a generation-dependent manner. In contrast, no significant distributional differences between same generation of DPK and DPO were observed, although the constituent amino acids, particle size, and zeta-potential were different. However, PEGylation of KG6 caused great changes in particle size, zeta-potential, blood retention and organ distribution in vivo, indicating that the PEGylation is applicable strategy to improve biodistribution characteristics of dendrimeric molecules. The information provided by this study will be helpful for the development of future drug delivery systems using amino acid dendrimers as safe drug carriers.

Keywords: Amino acid dendrimer; Biodistribution; Drug delivery system; Nano-carrier; PEGylation

1. Introduction

In spite of having excellent pharmacological effects, many drugs, especially most anticancer drugs, are limited in their clinical application due to a number of factors, including unfavorable biodistribution, serious toxicity, and poor water solubility. Therefore, in order to improve the biodistribution characteristics, suppress any harmful side effects, and enhance beneficial pharmacological effects, many research teams around the world are developing drug formulations, which can deliver pharmacologically active drugs to their target sites with high efficiency. In this field, several kinds of synthetic macromolecules have been developed and investigated as drug carriers [1–5]. Hence, the development of more functional drug carrier molecules is essential to attain a more targeted delivery of drugs.

To date, emulsions [6–8], liposomes [9–11], and polymeric micelles [12–14] have been developed as drug carriers. Since these carriers consist of amphiphilic molecules, they have a broad size distribution. In contrast, dendrimers have attracted great attention as far as biomedical application is concerned [15,16]. Dendrimers are unique highly branched spherical

Abbreviations: DPKs, dendritic poly(L-lysine)s; DPOs, dendritic poly(L-ornithine)s; KG6, the sixth generation of DPK; PAMAM, poly(amidoamine); Boc, *t*-butoxycarbonyl; DCHA, dicyclohexyl amine; HBTU, 2-(1*H*-benzotriazole-1-yl)-1,1,3,3-tetramethyluronium hexafluorophosphate; HOBt, 1-hydroxybenzotriazol; TFA, trifluoroacetic acid; DTPA, diethylenetriamine-*N*,*N*,*N*′,*N*″,*N*″-pentaacetic acid; MALDI TOF-MS, matrix-assisted time of flight mass spectrometry; DMF, *N*,*N*-dimethylformamide; PBS, phosphate-buffered saline; MWCO, molecular weight cut-off.

* Corresponding author. Tel.: +81 75 753 4525; fax: +81 75 753 4575.
E-mail address: hashidam@pharm.kyoto-u.ac.jp (M. Hashida).

0168-3659/$ - see front matter © 2006 Elsevier B.V. All rights reserved.
doi:10.1016/j.jconrel.2006.05.009

polymers with a narrow size distribution due to their distinctive method of synthesis (i.e., stepwise elongation of their generation). Monodispersed molecules like dendrimers would enable us to achieve more precise drug delivery. Therefore, dendrimers are potentially important candidates for the development of novel drug delivery systems. Poly(amidoamine) (PAMAM) dendrimer is a typical dendrimer. PAMAM dendrimers are commercially available macromolecules that can be used as carriers for plasmid DNA, antisense oligonucleotide and siRNA [17–21]. Moreover, PAMAM dendrimers are being investigated not only for gene therapy but also for drug delivery and bioimaging purposes [22,23]. However, Malik et al. have reported that PAMAM dendrimers exhibit generation-dependent cytotoxicity [24]. Furthermore, the mechanism of cell death induced by cationic PAMAM dendrimers has been reported by Kuo et al. [25]. Therefore, the work described here is intended to allow for the development of safer dendritic carrier molecules.

Dendritic poly(L-lysine)s (DPKs), which consist of amino acids, are also dendrimers that have different branch units compared with PAMAM-type dendrimers. Recently, we have reported that DPKs, especially its sixth generation (KG6), exhibit a high gene transfection ability in several kinds of cultivated cells without any significant cytotoxicity [26]. We also found that the KG6 had a protective effect against the degradation of plasmid DNA from endonucleases in blood in vivo, so that DPKs are expected to be good gene carrier not only in vitro but also in vivo [27]. DPKs can be synthesized with a well-defined structure and a precise number of surface amino groups per dendrimer. In addition, DPKs can easily alter their size and physicochemical properties by changing the constituent amino acid [28] and their surface amino groups can be modified by means of several functional groups, such as sugar chains, antibodies and so on. Therefore, amino acid dendrimers are important candidates for safer drug delivery systems.

When the newly developed material is used as a drug carrier, it is necessary to evaluate its own biodistribution characteristics. However, the in vivo disposition of amino acid dendrimers administered intravenously has not yet been investigated. In order to clarify the relationship between the physicochemical parameters and biodistribution characteristics of amino acid dendrimers, we synthesized several generations of DPKs and dendritic poly(L-ornithine)s (DPOs), which are composed of L-ornithine, and investigated their size, zeta-potential and disposition in mice after intravenous administration. Moreover, since there is no report in which the effect of PEGylation on the biodistribution characteristics of dendrimeric drug carriers has been discussed, we also prepared PEGylated KG6, and discuss them in the same way.

2. Materials and methods

2.1. Chemicals and instruments

Di-*t*-butyl dicarbonate (Boc_2O) was purchased from Peptide Institute, Inc. (Osaka, Japan). Organic solvents used in all synthesis procedures, lysine and ornithine monohydrochloride, ethylenediamine, hexamethylenediamine, and transaminase CII-test Wako were purchased from Wako Pure Chemical Industries, Ltd. (Osaka, Japan). The sixth generation of PAMAM dendrimer (PAMAM-G6) was purchased from SIGMA-ALDRICH Corporation (St. Louis, USA). Trifluoroacetic acid, dicyclohexyl amine (DCHA), and triethylamine were purchased from Nacalai Tesque, Inc. (Kyoto, Japan). The coupling reagents, 2-(1*H*-benzotriazole-1-yl)-1,1,3,3-tetramethyluronium hexafluorophosphate (HBTU) and 1-hydroxybenzotriazol (HOBt), were purchased from Novabiochem, Merck Ltd. (Tokyo, Japan). DTPA anhydride was purchased from Dojindo (Kumamoto, Japan). The $^{111}InCl_3$ was kindly provided by Nihon Medi-Physics Co. Ltd. (Hyogo, Japan). Mass spectra were obtained by matrix-assisted time of flight mass spectrometry (MALDI TOF-MS) using an Applied Biosystems, Voyager Linear DE instrument (Tokyo, Japan).

2.2. Synthesis of amino acid dendrimers

Lysine or ornithine monohydrochloride was dissolved in distilled water, and then Boc_2O in dioxane was added. The pH of the reaction mixture was adjusted to 8.0 or above by addition of 1 M NaOH. After overnight stirring at room temperature, dioxane was evaporated and the product was extracted with ethylacetate. The organic phase was washed three times with 10% citric acid and saturated NaCl, respectively, and then evaporated. *N*-Boc-protected lysine and ornithine were crystallized from petroleum ether with an equivalent molar ratio of DCHA. DPKs and DPOs were synthesized according to a method reported previously [26]. In brief, for the first generation synthesis, *N*-Boc-protected lysines or ornithines were coupled with diamines (hexamethylenediamine for DPKs or ethylenediamine for DPOs) in DMF by the HBTU-HOBt method [29], and then deprotection was performed by TFA treatment. For the synthesis of the second and higher generations, the coupling reaction between the amino group-free previous generation of dendrimers and *N*-Boc-protected lysines or ornithines was performed in DMF by the HBTU-HOBt method and, subsequently, Boc-groups were removed by TFA. We synthesized dendrimers up to the sixth generation by repetition of these coupling and deprotection procedures. The molecular weights of these synthesized dendrimers were measured by MALDI-TOF MS.

2.3. Evaluation of physicochemical properties of amino acid dendrimers

The fourth and further generations of dendrimers were suspended in PBS (pH 7.3) at a concentration of up to 5 mg/ml, and then their particle size and zeta-potential were measured by Zetasizer Nano ZS (Malvern Instruments Ltd., United Kingdom).

2.4. Radiolabeling of amino acid dendrimers

For the biodistribution experiments, each generation of amino acid dendrimers was radiolabeled with ^{111}In using the

bifunctional chelating agent, DTPA anhydride, according to the method of Hnatowich et al. [30]. This radiolabeling method is suitable for examining the biodistribution of macromolecules from plasma to various tissues because the radioactive metabolites, if produced after cellular uptake, are retained within the cells where the uptake takes place [31,32]. In brief, the amino acid dendrimer was dissolved in 20 mM borate buffer (pH 9.8) and DTPA anhydride in dimethyl sulfoxide was added at the molar ratio of 1:1. After mixing for 1 h at room temperature, the reaction mixture was purified by ultrafiltration using a VIVASPIN-20 (MWCO 3000 for the fourth generation or 5000 for the fifth and sixth generations). The purified DTPA-labeled dendrimer was then lyophilized, and the DTPA-labeled dendrimer solution was dissolved in 100 mM sodium citrate buffer (pH 5.5) at a concentration of 2 mg/ml. Twenty microliters $^{111}InCl_3$ solution was mixed with an equivalent volume of 100 mM sodium citrate buffer, and the mixture was allowed to stand for a few minutes. Then, 40 μl DTPA-labeled dendrimer solution was added and mixed well. After standing for 30 min at room temperature, the mixture was purified by gel filtration chromatography using a PD-10 column and eluted with sodium citrate buffer. The appropriate fractions were selected based on their radioactivity and concentrated by ultrafiltration using a VIVASPIN-20.

2.5. PEGylation of KG6

In order to prevent steric hindrance by PEG chains on the surface of dendrimer, the reaction between KG6 and DTPA anhydride was performed by the method described above before PEGylation. The DTPA-labeled KG6 was dissolved in borate buffer and reacted with PEG-NHS (Mw: 5000) at 4 °C. After overnight incubation, the reaction mixture was subjected to ultrafiltration using a VIVASPIN (MWCO 100,000). The degree of modification of the surface primary amino groups by PEG-NHS was evaluated by the barium–iodine method [33].

2.6. Animals

Male ddY mice (5 weeks old, 25–27 g) were purchased from Shizuoka Agricultural Co-Operative Association for Laboratory Animals (Shizuoka, Japan). Animals were maintained under conventional housing conditions. All animal experiments were performed according to the Guidelines for Animal Experimentation at Kyoto University.

2.7. Biodistribution experiment

^{111}In-labeled dendrimer was dissolved in saline, and the concentration of dendrimer was adjusted by addition of non-radiolabeled dendrimer to the solution. The ^{111}In-labeled dendrimer solution was administered via the tail vein to 5-week-old ddY mice at a dose of 1 mg/kg. At an appropriate time interval after intravenous injection, blood was collected from the vena cava under ether anesthesia and the mice were then sacrificed. The liver, kidneys, spleen, heart, and lungs were removed, rinsed with saline, blotted dry, and weighed. The collected blood was centrifuged for 5 min at 2000×*g* to obtain plasma. Samples of the collected organs and 100 μl plasma were transferred to counting tubes, and the radioactivity of each sample was measured using a gamma counter.

2.8. In vivo cytotoxicity analysis

The sixth generation of DPK and PAMAM dendrimer was administered via tail vein to 5-week-old ddY mice at three doses (1 mg/kg, 5 mg/kg, 10 mg/kg). Blood was collected at 24 h after administration. Serum was prepared by incubation of collected blood for 30 min at room temperature and centrifugation at 6000×*g* for 20 min at 4 °C. The serum glutamic pyruvic

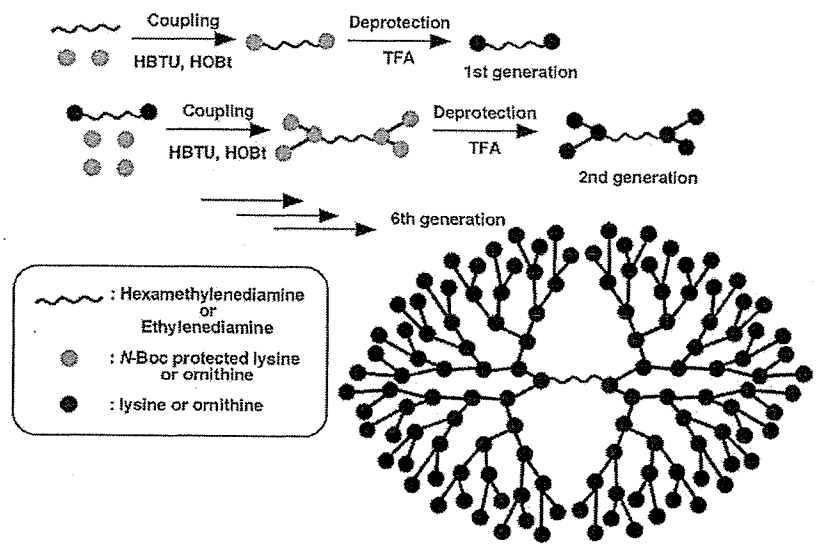

Fig. 1. Structure and synthetic route of amino acid dendrimers.

transaminase (GPT) activities were measured by using commercial kit (Transaminase CII-test Wako).

2.9. Statistical analysis

Statistical analysis was performed using Student's paired *t*-test for two groups. Multiple comparisons among different generations were made by Tukey–Kramer test or ANOVA with Dunnett's mean test. $P<0.05$ was considered to be indicative of statistical significance.

3. Results

3.1. Synthesis of amino acid dendrimers

The structures of DPKs and DPOs, a novel type of amino acid dendrimer, are shown in Fig. 1. DPKs and DPOs were synthesized from hexamethylenediamine or ethylenediamine as the initiator core, respectively. The first generation of each of the amino acid dendrimers was synthesized by coupling *N*-Boc-protected lysine or ornithine to the core molecule by the HBTU-HOBt method [29]. The second to sixth generations of each of the amino acid dendrimers were obtained by repetition of coupling and deprotection with TFA. After every coupling step, the amino acid dendrimers were purified by extraction or gel chromatography. The first to sixth generations of DPKs and DPOs were named KG1 to KG6 and OG1 to OG6, respectively. The final preparations of the fourth and further dendrimers were identified by MALDI TOF-MS (data not shown).

3.2. Physicochemical properties of amino acid dendrimers

The physicochemical properties of amino acid dendrimers were analyzed by a Zetasizer Nano ZS (Table 1). The mean diameter of KG4 to KG6 was about 3.41, 4.70, and 5.85 nm, respectively. On the other hand, the mean particle size of OG4 to OG6 was about 3.20, 3.96, and 5.22 nm, respectively. The particle size of each series of dendrimers increased gradually depending on their generation. All amino acid dendrimers subjected to zeta-potential analysis had a slightly positive potential and their surface charge gradually increased with their generation. DPKs were slightly larger with a higher zeta-potential than DPOs of the same generation.

Table 1
Physicochemical properties of amino acid dendrimers in PBS

	Molecular Weight	Number of $-NH_2$ groups	Particle size (nm)	Zeta-potential (mV)
KG4	3962	32	3.41±0.13	14.86±0.73
KG5	8065	64	4.70±0.04	17.31±4.54
KG6	16,269	128	5.85±0.06	19.77±0.30
OG4	3485	32	3.20±0.06	6.52±0.58
OG5	7139	64	3.96±0.08	9.49±0.33
OG6	14,446	128	5.22±0.03	9.33±0.46

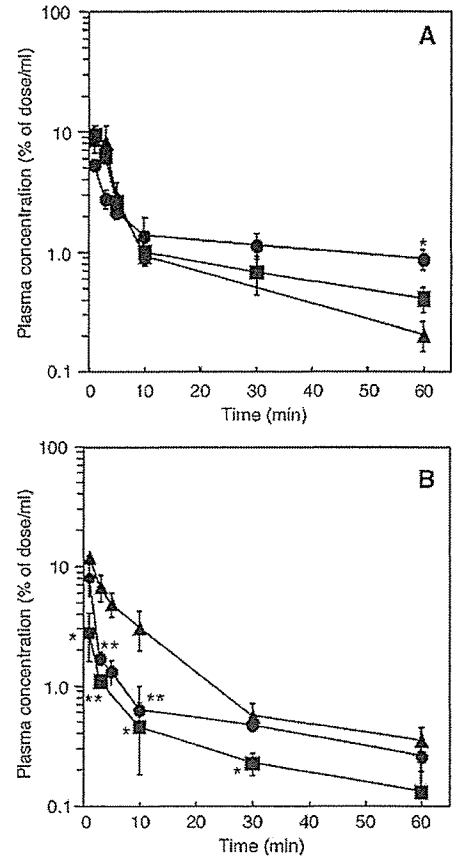

Fig. 2. Plasma concentration of ^{111}In-labeled DPKs (A) and DPOs (B) after intravenous administration to mice at a dose of 1 mg/kg. The fourth (▲), fifth (■), and sixth (●) generation of amino acid dendrimers were subjected to biodistribution experiments. Each value represents the mean±S.D. of three experiments. Statistically significant differences compared with the fourth generation (*$P<0.05$; **$P<0.01$) or the fifth generation (†$P<0.05$; ††$P<0.01$).

3.3. Plasma concentration of ^{111}In-labeled amino acid dendrimers

Fig. 2 shows the plasma concentration profiles of ^{111}In-labeled DPKs (A) and DPOs (B) after intravenous injection into mice up to 60 min. All amino acid dendrimers were rapidly eliminated from blood circulation within a few minutes, indicating that the amino acid dendrimer rapidly accumulated in some organs or was excreted into urine and feces. Although the particle size (generation), zeta-potential, and the constituent amino acids were different, no significant differences in the blood concentration profiles of the ^{111}In-labeled amino acid dendrimers were observed.

3.4. Tissue distribution of ^{111}In-labeled amino acid dendrimers

The biodistribution characteristics of the amino acid dendrimers were evaluated up to 60 min post-intravenous injection into mice by measuring the radioactivity in the liver, kidney, spleen, heart, lung, and urine. Regardless of the constituent amino acid and its generation, most of the amino

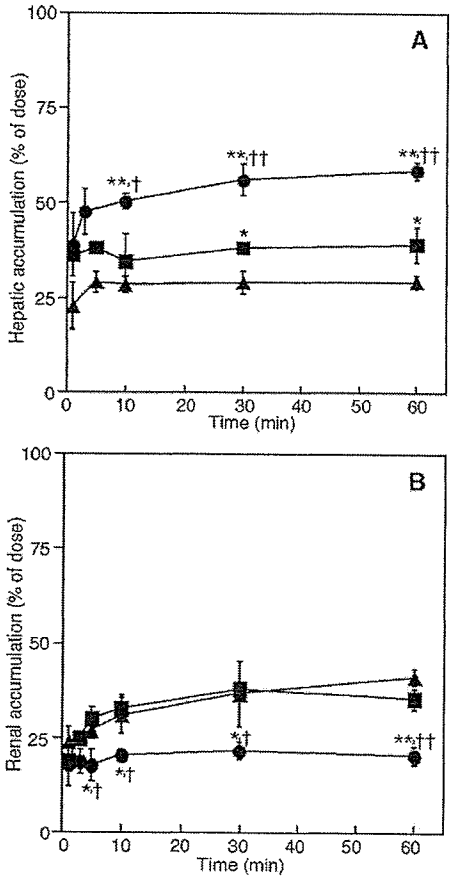

Fig. 3. Hepatic (A) and renal (B) accumulation of ^{111}In-labeled DPKs after intravenous administration to mice at a dose of 1 mg/kg. The fourth (▲), fifth (■), and sixth (●) generation of DPKs were subjected to biodistribution experiments. Each value represents the mean±S.D. of three experiments. Statistically significant differences compared with the fourth generation (*P<0.05; **P<0.01) or the fifth generation (†P<0.05; ††P<0.01).

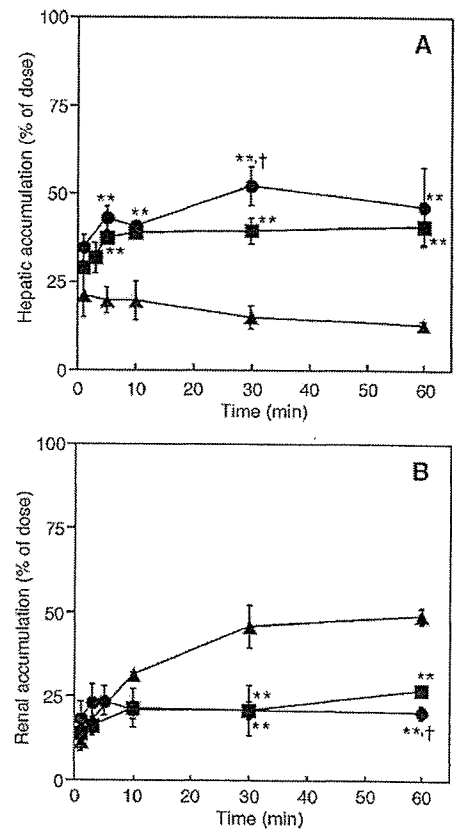

Fig. 4. Hepatic (A) and renal (B) accumulation of ^{111}In-labeled DPOs after intravenous administration to mice at a dose of 1 mg/kg. The fourth (▲), fifth (■), and sixth (●) generation of DPOs were subjected to biodistribution experiments. Each value represents the mean±S.D. of three experiments. Statistically significant differences compared with the fourth generation (*P<0.05; **P<0.01) or the fifth generation (†P<0.05; ††P<0.01).

acid dendrimers were recovered from the liver and kidney. The hepatic and renal accumulation profiles of DPKs and DPOs are shown in Figs. 3 and 4, respectively. The hepatic disposition of both DPKs and DPOs gradually increased in a generation-dependent manner (Figs. 3A and 4A). However, the higher the generation, the lower the renal accumulation of dendrimer (Figs. 3B and 4B). Also, no significant difference between the same generation of DPK and DPO was observed as far as both hepatic and renal accumulation were concerned. In contrast, all dendrimers investigated were virtually never detected in the spleen, heart, lung, and urine (data not shown).

3.5. In vivo cytotoxicity of dendrimers

To investigate in vivo cytotoxicity of KG6 and PAMAM dendrimer, serum GPT activity was measured at 24 h post-administration (Fig. 5). As a result, the serum GPT activities of KG6- or PAMAM-G6-treated mice were slightly increased with dose-dependent manner compared with saline treatment group. However, these values were within normal levels,

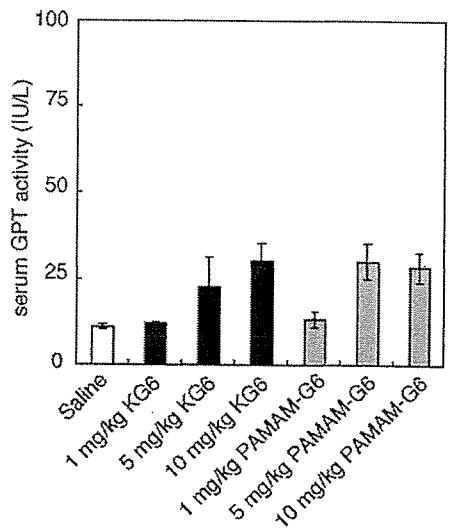

Fig. 5. The serum GPT activities at 24 h after intravenous administration of KG6 and PAMAM-G6 at three doses (1 mg/kg, 5 mg/kg, 10 mg/kg). Each value represents the mean±S.D. of three experiments. Statistically significant differences (*P<0.05) between saline treatment group and three doses of KG6 or PAMAM-G6 were analyzed by ANOVA with Dunnett's multiple comparison of means test.

Table 2
Physicochemical properties of PEGylated KG6 in PBS

	Number of PEG_{5000} [a]	Number of $-NH_2$ groups [b]	Particle size (nm)	Zeta-potential (mV)
KG6	0	128	5.85±0.06	19.77±0.30
PEG-KG6	76.2	51.8	16.92±0.13	−6.51±0.18

[a] The number of PEG_{5000} was determined by the barium–iodine method.
[b] The number of surface amino groups was determined by subtracting the result of the barium–iodine method from the number of native KG6's surface amino groups.

suggesting that KG6 and PAMAM-G6 showed no significant acute hepatic damages even at the dose of 10 mg/kg.

3.6. Surface modification of KG6 with polyethylene glycol chain

In order to investigate the influence of surface modification of the amino acid dendrimer in terms of its biodistribution, PEGylation of KG6 was performed. The degree of modification of PEGylated-KG6 was evaluated by the barium–iodine method [33], and found to be 59.5%. The particle size and zeta-potential of PEGylated-KG6 were measured (Table 2). The particle size increased about 2.5-fold compared with intact KG6, and the zeta-potential shifted from positive to slightly negative.

3.7. Plasma concentration of ^{111}In-labeled PEGylated KG6

PEGylated-KG6 was subjected to a biodistribution experiment identical to that for other surface non-modified amino acid dendrimers. The plasma concentration profile of intravenously administered ^{111}In-labeled PEGylated-KG6 up to 60 min is shown in Fig. 6A. The retention time in the blood was dramatically enhanced by PEGylation of KG6. Furthermore, about 20% of the injected dose was recovered from plasma even at 24 h after intravenous injection (Fig. 6B).

3.8. Tissue distribution of ^{111}In-labeled PEGylated KG6

PEGylated-KG6 also scarcely accumulated in the spleen, heart, lung, and urine like other intact amino acid dendrimers. The hepatic accumulation of PEGylated-KG6 was significantly lower compared with KG6 (Fig. 7A). On the other hand, no renal accumulation of PEGylated-KG6 was detected (Fig. 7B).

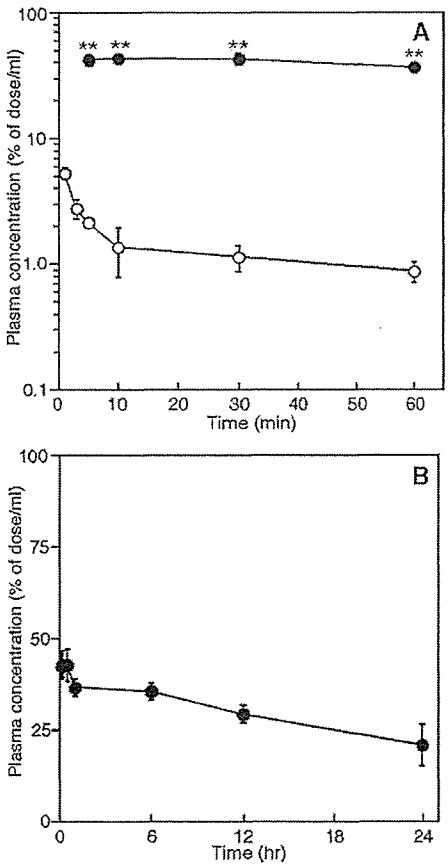

Fig. 6. The short-term (A) and long-term (B) plasma concentration profiles of ^{111}In-labeled PEGylated KG6 after intravenous administration to mice at a dose of 1 mg/kg. Each value represents the mean±S.D. of three experiments. Closed and open circles represent plasma concentration profiles of PEGylated KG6 and intact KG6, respectively. Statistically significant differences (*$P<0.05$; **$P<0.01$) between PEGylated KG6 and intact KG6 at each time point.

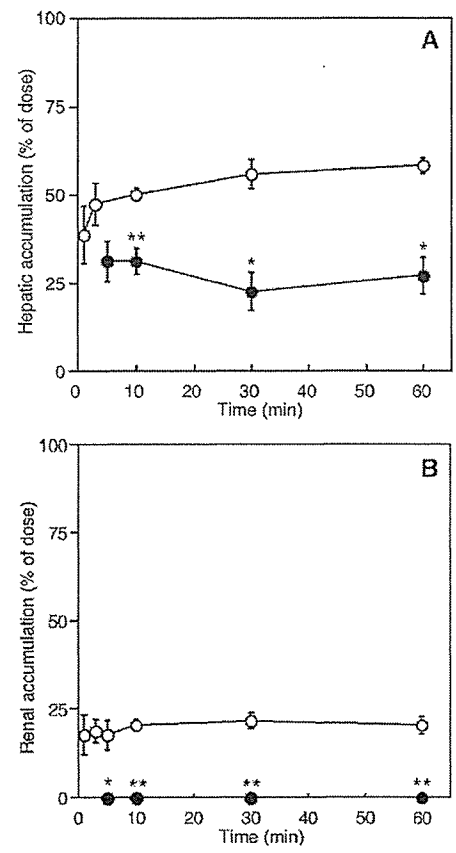

Fig. 7. Hepatic (A) and renal (B) accumulation of ^{111}In-labeled PEGylated KG6 after intravenous administration to mice at a dose of 1 mg/kg. Each value represents the mean±S.D. of three experiments. Closed and open circle represent biodistribution profiles of PEGylated KG6 and intact KG6, respectively. Statistically significant differences (*$P<0.05$; **$P<0.01$) between PEGylated KG6 and intact KG6 at each time point.

4. Discussion

Dendrimers can be synthesized with well-controlled size in nanometer properties. We easily obtained derivatives of amino acid dendrimers that had different particle sizes, zeta-potentials, and physicochemical and biological properties by altering the constituent amino acid and/or modifying surface amino groups with several functional groups [28]. Furthermore, our previous report demonstrated that DPKs are important candidates for safer carriers [26]. Therefore, we expect amino acid dendrimers to be promising basic materials for the development of safer carrier systems in the field of nano-medicine and focused on DPKs. In addition to DPKs, DPOs and PEGylated KG6 were synthesized to investigate the effect of generation, and physicochemical properties on their distribution after intravenous administration.

Since physicochemical properties, such as particle size and zeta-potential, are important factors controlling the biodistribution characteristics [34], we measured these two parameters. Both DPKs and DPOs could be synthesized with well-controlled size in nanometer properties (Table 1). The DPOs were smaller in size than the same generation of DPKs. This observation agrees with the fact that the side chain of ornithine is shorter than that of lysine. The zeta-potentials of all amino acid dendrimers examined in this study were slightly positive and increased in a generation-dependent manner. However, the zeta-potential of DPOs was lower compared with same generation of DPKs (Table 1). The reason for this difference in zeta-potential may be due to the fact that the protonation of surface amino group may be inhibited to suppress the charge repulsion caused by the high density of surface primary amino groups of DPOs, which have a more compact structure compared with the same generation of DPKs.

As shown in Figs. 2–4, all dendrimers investigated were rapidly eliminated from the blood and accumulated in mainly the liver and kidney. Unexpectedly, OG4 showed, however, substantially slower clearance from blood stream in the initial elimination phase compared with OG5 and OG6 (Fig. 2B). Maybe this unforeseen behavior of OG4 is due to its lower accumulation than the fifth and sixth generation of DPOs into liver and kidney in the early phase (Fig. 4). Although lung and spleen are a part of reticulo-endothelial system (RES) known to be involved in clearing macromolecule, no significant accumulation was observed not only in the heart and urine but also in lung and spleen. This reason why is mostly due to very rapid elimination of intravenously injected DPKs and DPOs from the blood stream (Fig. 2). The amount of hepatic accumulation increased in a generation-dependent manner (Figs. 3A and 4A). This increment in hepatically distributed dendrimer is caused by an increase in the surface positive charge in parallel with the generation increment. The kidney plays an important role in the clearance of macromolecules circulating in the bloodstream. Macromolecules with a molecular weight less than 50,000 (approximately 6 nm in diameter) are susceptible to glomerular filtration and are excreted in the urine [35]. Interestingly, although all the amino acid dendrimers used in this study have a subliminal molecular weight of glomerular filtration (Table 1), the dendrimers accumulated in kidney without any significant urinary excretion (Figs. 3B and 4B). We previously reported that cationic macromolecules, such as diethylaminoethyl-dextran (DEAE-dextran) and cationized BSA, are taken up by kidney from the capillary side based on electrostatic interactions and are distributed to both the medulla and cortex region [36]. The same phenomenon might have been caused by the highly concentrated positive charge on the surface of the amino acid dendrimers.

Since intravenously administered amino acid dendrimers rapidly accumulated into the liver, it was a concern that hepatically accumulated dendrimers might cause acute hepatic damages. Therefore, the serum GPT activity was measured at 24 h after administration. The serum GPT activities of KG6- or PAMAM-G6-treated mice were dose-dependently increased (Fig. 5). However, these values were within normal levels. Moreover, because the serum GPT level reached at several hundreds or thousands IU/L when the acute hepatic damages were induced by CCl_4-treatment, serum GPT activities observed at 24 h post-administration were considered to be significantly lower levels even at the dose of 10 mg/kg. In this experiment, the sixth generation of PAMAM dendrimer also showed no significant hepatic toxicity. Hence, both KG6 and PAMAM-G6 might have no acute hepatic toxicity. However, since the in vitro cytotoxicity of PAMAM dendrimers have been reported [24,25], we are convinced that amino acid dendrimers are safer than PAMAM dendrimers.

Polyethylene glycol (PEG), which is a biocompatible material, could improve the biodistribution by suppressing any unfavorable non-specific interaction with biomolecules. In order to confirm the effect of PEGylation on the disposition of amino acid dendrimers, PEGylation of KG6 was performed and the biodistribution characteristics of PEGylated-KG6 were evaluated. The particle size increased about 2.5-fold compared with intact KG6 and the zeta-potential shifted from positive to slightly negative following surface modification of KG6 with PEG chains (Table 2). As shown in Fig. 6, PEGylation of KG6 substantially enhanced blood retention, compared with that of intact KG6. Furthermore, the PEGylation reduced hepatic accumulation and almost completely abolished renal accumulation (Fig. 6). These results well agree with reports that PEGylation of drug carriers such as liposome and other polymer could improve their biodistribution characteristics by reducing non-specific interaction with biomolecules. This finding is strongly suggesting that PEGylation is also able to improve the biodistribution properties of the dendrimeric drug carriers such as amino acid dendrimers.

In conclusion, we synthesized DPKs, DPOs, and PEGylated KG6 and evaluated the effect of generation and physicochemical properties on biodistribution after intravenous administration. Although each amino acid dendrimer has a different particle size and zeta-potential at the same generation, no significant difference in the biodistribution characteristics of the amino acid dendrimers was observed. However, the hepatic and

renal accumulation was altered in a generation-dependent manner. Moreover, PEGylation of the dendrimers dramatically changed their disposition in vivo, suggesting that the PEGylation is also useful strategy to improve biodistribution characteristics of dendrimeric drug carriers. Our findings should be helpful for the exploitation of amino acid dendrimers as future drug delivery carriers.

Acknowledgements

This work was supported in part by Grants-in-Aid for Scientific Research from the Ministry of Education, Culture, Sports, Science, and Technology of Japan, and by the Health and Labour Sciences Research Grants for Research on Advanced Medical Technology from the Ministry of Health, Labour and Welfare of Japan.

We acknowledge the operation of the MALDI TOF-MS by Mr. Ryosuke Kurihara in the Department of Applied Chemistry, Faculty of Engineering, Kyushu University, Fukuoka, Japan.

References

[1] T. Etrych, M. Jelinkova, B. Rihova, K. Ulbrich, New HPMA copolymers containing doxorubicin bound via pH-sensitive linkage: synthesis and preliminary in vitro and in vivo biological properties, J. Control. Release 73 (2001) 89–102.

[2] M. Ozeki, T. Ishii, Y. Hirano, Y. Tabata, Controlled release of hepatocyte growth factor from gelatin hydrogels based on hydrogel degradation, J. Drug Target. 9 (2001) 461–471.

[3] T. Kushibiki, K. Matsumoto, T. Nakamura, Y. Tabata, Suppression of the progress of disseminated pancreatic cancer cells by NK4 plasmid DNA released from cationized gelatin microspheres, Pharm. Res. 21 (2004) 1109–1118.

[4] M. Higaki, T. Ishihara, N. Izumo, M. Takatsu, Y. Mizushima, Treatment of experimental arthritis with poly(D,L-lactic/glycolic acid) nanoparticles encapsulating betamethasone sodium phosphate, Ann. Rheum. Dis. 64 (2005) 1132–1136.

[5] T. Takahashi, Y. Yamada, K. Kataoka, Y. Nagasaki, Preparation of a novel PEG-clay hybrid as a DDS material: dispersion stability and sustained release profiles, J. Control. Release 107 (2005) 408–416.

[6] P.J. Stevens, R.J. Lee, A folate receptor-targeted emulsion formulation for paclitaxel, Anticancer Res. 23 (2003) 4927–4931.

[7] J. Han, S.S. Davis, C. Papandreou, C.D. Melia, C. Washington, Design and evaluation of an emulsion vehicle for paclitaxel: I. Physicochemical properties and plasma stability, Pharm. Res. 21 (2004) 1573–1580.

[8] W. Yeepare, S. Kawakami, Y. Higuchi, F. Yamashita, M. Hashida, Biodistribution characteristics of mannosylated and fucosylated O/W emulsions in mice, J. Drug Target. 13 (2005) 1–9.

[9] H. Harashima, S. Iida, Y. Urakami, M. Tsuchihashi, H. Kiwada, Optimization of antitumor effect of liposomally encapsulated doxorubicin based on simulations by pharmacokinetic/pharmacodynamic modeling, J. Control. Release 61 (1999) 93–106.

[10] S. Kawakami, J. Wong, A. Sato, Y. Hattori, F. Yamashita, M. Hashida, Biodistribution characteristics of mannosylated, fucosylated, and galactosylated liposomes in mice, Biochim. Biophys. Acta 1524 (2000) 258–265.

[11] X. Guo, F.C. Szoka Jr., Steric stabilization of fusogenic liposomes by a low-pH sensitive PEG-diortho ester-lipid conjugate, Bioconjug. Chem. 12 (2001) 291–300.

[12] A.N. Lukyanov, V.P. Torchilin, Micelles from lipid derivatives of water-soluble polymers as delivery systems for poorly soluble drugs, Adv. Drug Deliv. Rev. 56 (2004) 1273–1289.

[13] Y. Bae, N. Nishiyama, S. Fukushima, H. Koyama, M. Yasuhiro, K. Kataoka, Preparation and biological characterization of polymeric micelle drug carriers with intracellular pH-triggered drug release property: tumor permeability, controlled subcellular drug distribution, and enhanced in vivo antitumor efficacy, Bioconjug. Chem. 16 (2005) 122–130.

[14] S. Kawakami, P. Opanasopit, M. Yokoyama, N. Chansri, T. Yamamoto, T. Okano, F. Yamashita, M. Hashida, Biodistribution characteristics of all-trans retinoic acid incorporated in liposomes and polymeric micelles following intravenous administration, J. Pharm. Sci. 94 (2005) 2606–2615.

[15] R. Esfand, D.A. Tomalia, Poly(amidoamine) (PAMAM) dendrimers: from biomimicry to drug delivery and biomedical applications, Drug Discov. Today 6 (2001) 427–436.

[16] S.E. Stibira, H. Frey, R. Haag, Dendritic polymers in biomedical applications: from potential to clinical use in diagnostics and therapy, Angew. Chem., Int. Ed. 41 (2002) 1329–1334.

[17] H. Yoo, P. Sazani, R.L. Juliano, PAMAM dendrimers as delivery agents for antisense oligonucleotides, Pharm. Res. 16 (1999) 1799–1804.

[18] H. Yoo, R.L. Juliano, Enhanced delivery of antisense oligonucleotides with fluorophore-conjugated PAMAM dendrimers, Nucleic Acids Res. 28 (2000) 4225–4231.

[19] J.S. Choi, K. Nam, J.Y. Park, J.B. Kim, J.K. Lee, J.S. Park, Enhanced transfection efficiency of PAMAM dendrimer by surface modification with L-arginine, J. Control. Release 99 (2004) 445–456.

[20] K. Wada, H. Arima, T. Tsutsumi, F. Hirayama, K. Uekama, Enhancing effects of galactosylated dendrimer/alpha-cyclodextrin conjugates on gene transfer efficiency, Biol. Pharm. Bull. 28 (2005) 500–505.

[21] H. Kang, R. Delong, M.H. Fisher, R.L. Juliano, Tat-conjugated PAMAM dendrimers as delivery agents for antisense and siRNA oligonucleotides, Pharm. Res. 22 (2005) 2099–2106.

[22] H. Kobayashi, S. Kawamoto, R.A. Star, T.A. Waldmann, Y. Tagaya, M.W. Brechbiel, Micro-magnetic resonance lymphangiography in mice using a novel dendrimer-based magnetic resonance imaging contrast agent, Cancer Res. 63 (2003) 271–276.

[23] H. Kobayashi, S.K. Jo, S. Kawamoto, H. Yasuda, X. Hu, M.V. Knopp, M. W. Brechbiel, P.L. Choyke, R.A. Star, Polyamine dendrimer-based MRI contrast agents for functional kidney imaging to diagnose acute renal failure, J. Magn. Reson. Imaging 20 (2004) 512–518.

[24] N. Malik, R. Wiwattanapatapee, R. Klopsch, K. Lorenz, H. Frey, J.W. Weener, E.W. Meijer, W. Paulus, R. Duncan, Dendrimers: relationship between structure and biocompatibility in vitro, and preliminary studies on the biodistribution of ^{125}I-labelled polyamidoamine dendrimers in vivo, J. Control. Release 65 (2000) 133–148.

[25] J.H. Kuo, M.S. Jan, H.W. Chiu, Mechanism of cell death induced by cationic dendrimers in RAW 264.7 murine macrophage-like cells, J. Pharm. Pharmacol. 57 (2005) 489–495.

[26] M. Ohsaki, T. Okuda, A. Wada, T. Hirayama, T. Niidome, H. Aoyagi, In vitro gene transfection using dendritic poly(L-lysine), Bioconjug. Chem. 13 (2002) 510–517.

[27] T. Kawano, T. Okuda, H. Aoyagi, T. Niidome, Long circulation of intravenously administered plasmid DNA delivered with dendritic poly(L-lysine) in the blood flow, J. Control. Release 99 (2004) 329–337.

[28] T. Okuda, A. Sugiyama, T. Niidome, H. Aoyagi, Characters of dendritic poly(L-lysine) analogues with the terminal lysines replaced with arginines and histidines as gene carriers in vitro, Biomaterials 25 (2004) 537–544.

[29] C.G. Fields, D.H. Lloyd, R.L. Macdonald, K.M. Otteson, R.L. Noble, HBTU activation for automated Fmoc solid phase peptide synthesis, Pept. Res. 4 (1991) 95–101.

[30] D. Hnatowich, W.W. Layne, R.L. Childs, The preparation and labeling of DTPA-coupled albumin, J. Appl. Radiat. Isot. 12 (1982) 327–332.

[31] J.R. Duncan, M.J. Welch, Intracellular metabolilsm of indium-111-DTPA-labeled receptor targeted proteins, J. Nucl. Med. 34 (1993) 1728–1738.

[32] F. Staud, M. Nishikawa, K. Morimoto, Y. Takakura, M. Hashida, Disposition of radioactivity after injection of liver-targeted proteins

labeled with ^{111}In or ^{125}I. Effect of labeling on distribution and excretion of radioactivity in rats, J. Pharm. Sci. 88 (1999) 577–585.
[33] B. Skoog, Determination of polyethylene glycols 4000 and 6000 in plasma protein preparations, Vox Sang. 37 (1979) 345–349.
[34] Y. Takakura, M. Hashida, Macromolecular carrier systems for targeted drug delivery: pharmacokinetic considerations on biodistribution, Pharm. Res. 13 (1996) 820–830.
[35] B.M. Brenner, T.H. Hostetter, H.D. Humes, Glomerular permselectivity: barrier function based on discrimination of molecular size and charge, Am. J. Physiol. 234 (1978) F455–F460.
[36] K. Mihara, M. Mori, T. Hojo, Y. Takakura, H. Sezaki, M. Hashida, Disposition characteristics of model macromolecules in the perfused rat kidney, Biol. Pharm. Bull. 16 (1993) 158–162.

THE JOURNAL OF GENE MEDICINE
J Gene Med 2006; 8: 824–834.
Published online 20 April 2006 in Wiley InterScience (www.interscience.wiley.com) **DOI:** 10.1002/jgm.910

RESEARCH ARTICLE

Enhanced DNA vaccine potency by mannosylated lipoplex after intraperitoneal administration

Yoshiyuki Hattori
Shigeru Kawakami
Yan Lu
Kazumi Nakamura
Fumiyoshi Yamashita
Mitsuru Hashida*

Department of Drug Delivery Research, Graduate School of Pharmaceutical Sciences, Kyoto University, Sakyo-ku, Kyoto 606-8501, Japan

*Correspondence to:
Mitsuru Hashida, Department of Drug Delivery Research, Graduate School of Pharmaceutical Sciences, Kyoto University, Sakyo-ku, Kyoto 606-8501, Japan. E-mail: hashidam@pharm.kyoto-u.ac.jp

Received: 15 December 2005
Revised: 31 January 2006
Accepted: 1 February 2006

Abstract

Background Here we describe a novel DNA vaccine formulation that can enhance cytotoxic T lymphocyte (CTL) activity through efficient gene delivery to dendritic cells (DCs) by mannose receptor-mediated endocytosis.

Methods Ovalbumin (OVA) was selected as a model antigen for vaccination; accordingly, OVA-encoding pDNA (pCMV-OVA) was constructed to evaluate DNA vaccination. Mannosylated cationic liposomes (Man-liposomes) were prepared using cholesten-5-yloxy-*N*-{4-[(1-imino-2-D-thiomannosylethyl)amino]butyl}formamide (Man-C4-Chol) with cationic lipid. The potency of the mannosylated liposome/pCMV-OVA complex (Man-lipoplex) was evaluated by measuring OVA mRNA in $CD11c^+$ cells, CTL activity, and the OVA-specific anti-tumor effect after *in vivo* administration.

Results An *in vitro* study using DC2.4 cells demonstrated that Man-liposomes could transfect pCMV-OVA more efficiently than cationic liposomes via mannose receptor-mediated endocytosis. *In vivo* studies revealed that the Man-lipoplex exhibited higher OVA mRNA expression in $CD11c^+$ cells in the spleen and peritoneal cavity and provided a stronger OVA-specific CTL response than intraperitoneal (i.p.) administration of the conventional lipoplex and intramuscular (i.m.) administration of naked pCMV-OVA, the standard protocol for DNA vaccination. Pre-immunization with the Man-lipoplex provided much better OVA-specific anti-tumor effect than naked pCMV-OVA via the i.m. route.

Conclusions These results suggested that *in vivo* active targeting of DNA vaccine to DCs with Man-lipoplex might prove useful for the rational design of DNA vaccine. Copyright © 2006 John Wiley & Sons, Ltd.

Keywords gene therapy; DNA vaccine; mannosylated liposomes; non-viral vectors

Introduction

DNA vaccine, plasmid DNA (pDNA)-encoding antigen from a pathogen, is of great interest in gene therapy as a means of immunotherapy against refractory diseases such as cancer and viral infections because the administration of naked pDNA-encoding antigen proteins induces not only an antibody response, but also a potent cytotoxic T lymphocyte (CTL) response in animal models [1–3]. Recent immunological studies have demonstrated that gene transfection and subsequent activation of antigen-presenting cells (APCs), dendritic cells (DCs) and macrophages are important for efficient DNA

vaccine therapy [4–6]. Although some clinical trials involving melanoma, human imuunodeficiency virus, and HCV have been performed using topical administration of naked pDNA [7–9], the results are not good enough for clinical therapy. In order to overcome this problem, it is important to develop gene delivery carriers for *in vivo* APC-selective gene transfection.

In spite of the high transfection efficiency of viral vectors, they still need to be improved from the point of view of safety issues [10–12]. The use of non-viral vectors is one of the possible approaches for *in vivo* gene delivery because they are free from some of the risks inherent in these systems. Furthermore, the characteristics of non-viral vectors can be more easily modified than those of viral vectors. To achieve targeted gene delivery, a number of receptor-mediated gene delivery systems have been developed [13–16] including our carriers [17–22]. As far as *in vivo* selective gene delivery to APCs is concerned, mannose has been shown to be a promising ligand to target APCs because these cells have a large number of mannose receptors.

Recently, we have developed several types of macromolecular [18] and particulate [22,23] gene carriers for macrophage-selective gene transfection *in vivo*. Among them, cationic liposomes containing cholesten-5-yloxy-*N*-{4-[(1-imino-2-D-thiomannosylethyl)amino]butyl} formamide (Man-C4-Chol) are some of the most interesting potential gene transfection carriers [22,23] that can be efficiently recognized by mannose receptors on macrophages in liver. Man-C4-Chol exhibits bifunctional properties, i.e., an imino group for binding to pDNA via electrostatic interaction and a mannose residue for the cell-surface receptors in APCs [22]. Therefore, a high density of mannose residues can be provided on the liposome surface without affecting the binding of the cationic liposomes to pDNA. More recently, we have demonstrated that intravenously administrated pCMV-OVA complexed with mannosylated liposomes (Man-lipoplex) enhances MHC class I antigen presentation, but no measurable CTL response was observed [24], suggesting that not only cell-selective gene transfection but also enhanced transfection efficiency in DCs is needed for gene therapy.

Intraperitoneal (i.p.) administration has some advantages as far as the transfection efficacy to DCs by Man-lipoplex is concerned; this is because of (i) high accessibility to APCs in the peritoneal cavity and lymph nodes, (ii) long retention of the lipoplex, (iii) the presence of few biocomponents that reduce transfection activity, and (iv) the high capacity of the lipoplex solution. Taking these factors into consideration, i.p. administrated Man-lipoplex would enhance gene expression in APCs resulting in efficient DNA vaccine therapy. However, few reports are available on the effect of i.p. administered Man-lipoplex on DNA vaccine therapy.

The objective of this paper was to clarify the DNA vaccine potency after i.p. administration of Man-lipoplex. In the present study, ovalbumin (OVA)-encoding pDNA (pCMV-OVA) was selected as a model DNA vaccine. Using *in vitro* and *in vivo* experiments, the transfection efficacy to APCs was evaluated by measuring the OVA mRNA using quantitative reverse-transcription polymerase chain reaction (RT-PCR). After immunizing with Man-lipoplex, OVA-specific CTL responses and its antitumor effects against inoculated E.G7-OVA cells (OVA expressing cells), and its parental cell line, EL4 cells (OVA non-expressing cells), were also evaluated. The results obtained were compared with those of conventional lipoplex and naked pCMV-OVA.

Materials and methods

Materials

Cholesteryl chloroformate, HEPES, concanavalin A, G418, and immunogloblin G were obtained from Sigma Chemicals Inc. (St. Louis, MO, USA). *N*-[1-(2,3-Dioleyloxy)propyl]-*N*,*N*,*N*-trimethylammonium chloride (DOTMA) and *N*-(4-aminobutyl)carbamic acid *tert*-butyl ester were obtained from Tokyo Chemical Industry Co. (Tokyo, Japan). Dioleoylphosphatidylethanolamine (DOPE) was purchased from Avanti Polar Lipids, Inc. (Alabaster, AL, USA). pVAX I, fetal bovine serum (FBS), and Opti-MEM I® were obtained from Invitrogen Co. (Carlsbad, CA, USA). Anti-CD11c monoclonal antibody (N418)-labeled magnetic beads were purchased from Miltenyi Biotec Inc. (Auburn, CA, USA). Nucleic acid purification kit magextractor®-RNA was purchased from Toyobo Co., Ltd. (Osaka, Japan). The first strand cDNA synthesis kit for RT-PCR, Lightcycler™ faststart DNA master hybridization probes, and a Lightcycler™-Primer/Probes set for mouse β-actin were purchased from Roche Diagnostics Co. (Indianapolis, IN, USA). Primers/probes for OVA were purchased from Nihon Gene Research Labs Inc. (Miyagi, Japan). All other chemicals were of the highest purity available.

Animals

Female ICR mice (4–5 weeks old) and C57BL/6 mice (6–8 weeks old) were purchased from the Shizuoka Agricultural Cooperative Association for Laboratory Animals (Shizuoka, Japan). All animal experiments were carried out in accordance with the Principles of Laboratory Animal Care as adopted and promulgated by the US National Institutes of Health and the guideline for animal experiments of Kyoto University.

Cell line

DC2.4 cells, a cell line of murine dendritic cells (DCs, haplotype H-2b) [25], were kindly provided by Dr. K. L. Rock (University of Massachusetts Medical School, Worcester, MA, USA). The expression of mannose receptors in this cell line has been confirmed elsewhere [26]. Therefore, DC2.4 cells are a suitable model of DCs.

EL4 cells (ATCC: TIB-39) and E.G7-OVA cells (ATCC: CRL-2113) were purchased from the American Type Culture Collection (ATCC, Manassas, VA, USA) and maintained in Dulbecco's modified Eagle's medium supplemented with 10% FBS and RPMI 1640 supplemented with 10% FBS, 4.5 g/l glucose, 10 mM HEPES, 1 mM sodium pyruvate, 0.05 mM 2-mercaptoethanol and 0.4 mg/ml G418.

Synthesis of Man-C4-Chol and Gal-C4-Chol

Man-C4-Chol and Gal-C4-Chol were synthesized as described previously [19,22]. Briefly, *N*-(4-aminobutyl)-(cholesten-5-yloxyl)formamide (C4-Chol) was synthesized from cholesteryl chloroformate and *N*-(4-aminobutyl)carbamic acid *tert*-butyl ester. The C4-Chol was reacted with 5 equivalents of 2-imino-2-methoxyethyl-1-thiomannoside or 2-imino-2-methoxyethyl-1-thiogalactoside [27] in pyridine containing 1.1 equivalents of triethylamine for 24 h. After evaporation of the reaction mixture *in vacuo*, the resultant material was suspended in water and dialyzed against water for 48 h, and then lyophilized.

Construction and preparation of pCMV-OVA

pCMV-OVA was constructed by subcloning the EcoRI chicken egg albumin (ovalbumin) cDNA fragment from pAc-neo-OVA [28], which was kindly provided by Dr. M. J. Bevan (University of Washington, Seattle, WA, USA), into the polylinker of pVAX I. pCMV-OVA was amplified in the *E. coli* strain, DH5α, then isolated, and purified using a Qiagen plasmid giga kit (Qiagen GmbH, Hilden, Germany). The endotoxin in pCMV-OVA solution was removed by the Triton X-114 method.

Preparation of cationic liposomes

Liposomes were prepared using the method reported previously [19,22]. Briefly, DOTMA, Chol, and Man-C4-Chol or Gal-C4-Chol were mixed in chloroform at a molar ratio of 2:1:1:0, 2:1:0:1, and 2:2:0:0 to prepare Man-liposomes, Gal-liposomes, and cationic liposomes, respectively. Then, the mixture was dried, vacuum desiccated, and resuspended in sterile 20 mM HEPES buffer (pH 7.8) or 5% dextrose solution in a sterile test tube for *in vitro* and *in vivo* experiments, respectively. After hydration, the dispersion was sonicated for 5 min in a bath sonicator to produce liposomes and then sterilized by passing through a 0.45 μm filter (Nihon-Millipore Ltd., Tokyo, Japan).

Preparation of lipoplex for *in vitro* study

Lipoplex was prepared using the method reported previously [19,22]. Briefly, equal volumes of pCMV-OVA and stock liposome solution were diluted with Opti-MEM I® in 15 ml Falcon tubes. Then, pCMV-OVA solution was added rapidly to the surface of the liposome solution at a charge ratio (−/+) of 1.0 : 2.3 using a micropipette (Pipetman®, Gilson, Villier-le Bel, France) and the mixture was agitated rapidly by pumping it up and down twice in the pipette tip.

Preparation of lipoplex for *in vivo* study

All cationic liposome/pCMV-OVA complexes for *in vivo* experiments were prepared under the optimal conditions for cell-selective gene transfection as reported previously [29–31]. Briefly, equal volumes of pCMV-OVA and stock liposome solution were diluted with 5% dextrose in 15 ml tubes. Then, pCMV-OVA solution was added rapidly to the surface of the liposome solution using a micropipette and the mixture was agitated rapidly by pumping it up and down twice in the pipette tip. The mean particle sizes were measured by dynamic light scattering spectrophotometry (LS-900; Otsuka Electronics Co., Ltd., Osaka, Japan). The zeta-potential of the lipoplexes was measured by the laser-Doppler electrophoresis method with a Zetasizer Nano ZS (Malvern Instruments Ltd., Worcestershire, UK).

Uptake characteristics by DC2.4 cells

Uptake study was performed by the method reported previously [19,22]. Briefly, the DC2.4 cells were plated on a 24-well plate at a density of 0.65×10^5 cells/cm^2 and cultivated in 500 μl RPMI supplemented with 10% FBS. Twenty-four hours later, the culture medium was replaced with an equivalent volume of Hanks medium (Nissui Pharmaceutical Co., Ltd., Tokyo, Japan) containing 1 kBq/ml [^{32}P]-pCMV-OVA, 0.5 mg/ml cold pCMV-OVA and cationic liposomes at a charge ratio (−/+) of 1.0 : 2.3. After incubation for given time periods, the solution was quickly removed by aspiration, the cells were washed five times with ice-cold HBSS buffer and then solubilized in 0.3 M NaOH solution with 10% Triton X-100 (0.3 ml). The radioactivity was measured by liquid scintillation counting (LSC-500; Beckman, Inc., Tokyo, Japan) and the protein content was determined by a modification of the Lowry method. The effect of the presence of 0.125 mg/ml mannan was determined in the same system.

Transfection activity by DC2.4 cells

DC2.4 cells were seeded in 10.5 cm^2 dishes at a density of 0.65×10^5 cells/cm^2 in RPMI 1640 medium supplemented with 10% FBS. After 24 h in culture, the culture medium was replaced with Opti-MEM I® containing 0.5 μg/ml pCMV-OVA and cationic liposomes. Six hours later, the incubation medium was replaced again with RPMI 1640 supplemented with 10% FBS and incubated for an additional 6 h. Then, the cells were

scraped and suspended in 200 µl pH 7.4 phosphate-buffered saline (PBS). Total RNA was isolated from DC2.4 cells with MagExtractor MFX-2000 (Toyobo Co., Ltd., Osaka, Japan) and MagExtractor-RNA following the manufacturer's instructions. Reverse transcription of mRNA was carried out using a first strand cDNA synthesis kit as follows: total RNA was added to the oligo dT primer (0.8 µg/µl) solution, and incubated at 42 °C for 60 min with a program temperature control system PC-808 (Astec Co., Ltd., Fukuoka, Japan). Real-time PCR was performed using the Lightcycler™ quick system 350S (Roche Diagnostics Co., Indianapolis, IN, USA) with hybridization probes. Primer and hybridization probes for OVA cDNA were constructed as follows: primer, 5′-GCGTCTCTGAATTTAGGG-3′ (forward) and 5′-TACCCCTGATACTACAGTGC-3′ (reverse); hybridization probes, 5′-CTTCTGTATCAAGCACATCGCAACCAACG-3′-fluorescein isothiocyanate (FITC) and Lightcycler™-Red640 (LCRed)-5′-CGTTCTCTTCTTTGGCAGATGTGT-TTCCCC-3′. The PCR reaction for detection of the OVA gene was carried out in a final volume of 20 µl containing: (i) 2 µl DNA Master hybridization probes 10× (DNA Master hybridization probes kit); (ii) 1.6 µl 25 mM $MgCl_2$; (iii) 1.5 µl forward and reverse primers (final concentration 0.75 µM); (iv) 1 µl 2 µM FITC-labeled hybridization probes and 2 µl 2 µM LCRed-labeled probes (final concentrations 0.2 and 0.4 µM, respectively); (v) 5.4 µl H_2O; (vi) 5 ml cDNA or pCMV-OVA solution. For the mouse β-actin cDNA measurements, samples were prepared in accordance with the instruction manuals. After an initial denaturation step at 95 °C for 10 min, temperature cycling was initiated. Each cycle consisted of denaturation at 95 °C for 10 s, hybridization at 60 °C for 15 s, and elongation at 72 °C for 10 s. The fluorescent signal was acquired at the end of the hybridization step (F2/F1 channels). The total number of cycles performed was 40. The mRNA copy numbers were calculated for each sample from the standard curve using the instrument software ('Arithmetic Fit Point analysis' for the Lightcycler). Results were expressed as relative copy numbers calculated relative to β-actin mRNA (copy number of OVA mRNA/copy number of β-actin mRNA).

Quantification of OVA mRNA in CD11c$^+$ cells after i.p. administration by quantitative PCR

pCMV-OVA (100 µg) or lipoplex was injected via the i.p. route. Spleens and peritoneal cells were harvested 6 h after i.p. administration and single cell suspensions of spleen cells were prepared in ice-cold RPMI 1640 medium. Ice-cold RPMI 1640 medium (5 ml) was injected and then peritoneal cells were collected as a cell suspension in RPMI medium. Following this, red blood cells were removed by incubation with Tris-NH_4Cl solution for 10 min at room temperature. Positive selection of CD11c$^+$ cells was carried out by magnetic cell sorting with auto MACS (Miltenyi Biotec Inc., Auburn, CA, USA) following the manufacturer's instructions. Briefly, the cell suspension was incubated with PBS containing 1 mg/ml IgG to block the Fcγ receptors of macrophages. Then, CD11c$^+$ cells were labeled by incubating with anti-CD11c monoclonal antibody (N418)-labeled magnetic beads. After washing three times, CD11c$^+$ cells were collected by auto MACS. Total RNA was isolated from the recovered CD11c$^+$ cells with a MagExtractor MFX-2000 (Toyobo Co., Ltd., Osaka, Japan) and MagExtractor-RNA following the manufacturer's instructions. Reverse transcription and quantitative PCR of OVA and β-actin mRNA were performed as described in the section 'Transfection activity by DC2.4 cells'.

Induction of OVA-specific CTL

C57BL/6 mice were immunized with naked pCMV-OVA (50 or 100 µg) or lipoplexes by i.p., i.m., or intradermal (i.d.) administration three times at intervals of 2 weeks. Two weeks after the last immunization, the spleens of each group were harvested and a single cell suspension was prepared in ice-cold RPMI 1640 medium. Then, the spleen cells were resuspended in RPMI 1640 medium supplemented with 10% FBS and 2-mercaptoethanol. The recovered spleen cells were plated in a 25-cm flask at 5×10^6 cells/ml along with MMC and E.G7-OVA cells and treated for 1 h (100 µg/ml, 1 h). Four days after cultivation, non-adherent cells were harvested, washed, and plated with relevant or irrelevant target cells at effector/target (E/T) ratios of 100 : 1, 50 : 1, 25 : 1, and 12.5 : 1. The target cells were E.G7-OVA cells or their parental cell line, EL4 cells. The target cell (E.G7-OVA or EL4 cells) suspensions in RPMI medium (2.5×10^7 cells/ml) were incubated with ^{51}Cr (7.4 MBq/ml) for 1 h. Following incubation, the cells were washed five times and then resuspended at 2×10^5 cells/ml. The target cells (E.G7-OVA or EL4 cells; 2×10^4 cells) were added to each well of a 96-well microtiter plate, along with 2×10^6, 1×10^6, 5×10^5, or 2.5×10^5 spleen cells and the plates were mixed and incubated for 4 h at 37 °C and 5% CO_2 in an incubator. After further centrifugation, 100 µl supernatant was collected from each well and the radioactivity released was measured in a gamma counter. The percentage ^{51}Cr release was calculated as follows: specific lysis (%) = [(experimental ^{51}Cr release − spontaneous ^{51}Cr release)/(maximum ^{51}Cr release − spontaneous ^{51}Cr release)] × 100). The percentage OVA-specific ^{51}Cr release was calculated as (% of ^{51}Cr release from E.G7-OVA) − (% of ^{51}Cr release from EL4).

Evaluation of protection against transplanted tumor cells in mice

C57BL/6 mice were immunized three times by i.p. or i.m. administration of naked pCMV-OVA (100 µg) or lipoplex at 2-week intervals. Then 2 weeks after the last

immunization, E.G7-OVA (1×10^6) or EL4 (1×10^6) cells were inoculated subcutaneously (s.c.) into the back of the mice. The survival of the mice was monitored up to 100 days after inoculation of the E.G7-OVA or EL4 cells.

Results

Particle sizes and zeta-potentials of Man-lipoplexes

To investigate the physicochemical properties of lipoplexes, the particle size and zeta-potential of each lipoplex were evaluated. Both lipoplexes showed a clear-cut distribution pattern and the mean particle sizes of the Man-lipoplexes and conventional lipoplex were 114 ± 7.8 and 116 ± 11.5 nm ($n = 3$), respectively. Zeta-potential analysis showed that the zeta-potential of the Man-lipoplex and the conventional lipoplex at a charge ratio (−/+) of 1.0 : 2.3 was 62.1 ± 1.85 and 64.1 ± 1.74 mV ($n = 3$), respectively. These results show that there was almost no difference in physicochemical properties between the two complexes. The galactosylated lipoplex (Gal-lipoplex) also showed a similar size distribution and zeta-potential (data not shown).

Uptake characteristics of Man-lipoplex by DC2.4 cells *in vitro*

To evaluate the potency of the Man-lipoplex in terms of targeted delivery to DCs, the uptake of the lipoplexes and subsequent transfection to cells were evaluated. In this study, we used DC2.4 cells, a cell line derived from DCs, as a model DC expressing mannose receptors [26]. The [^{32}P] Man-lipoplex was taken up by DC2.4 cells more efficiently than the conventional [^{32}P] lipoplex (Figure 1a) and this was significantly reduced in the presence of an excess of mannan (Figure 1b). In contrast, the uptake with conventional lipoplex was not significantly inhibited by an excess of mannan (Figure 1b).

Transfection characteristics of Man-lipoplex with respect to DC2.4 cells *in vitro*

We next investigated the transfection activity of the Man-lipoplex with respect to DC2.4 cells. As shown in Figure 2a, the highest gene expression was observed in the Man-lipoplex. In the presence of an excess of mannan, the gene expression of the Man-lipoplex was significantly inhibited (Figure 2b). In contrast, the gene expression with conventional lipoplex and naked pDNA was not significantly inhibited in the presence of an excess of mannan (Figure 2b).

Effect of Man-lipoplex administration routes on CTL response

To investigate the effect of the administration route of the Man-lipoplex, the induction of an OVA-specific cytotoxic response with a ^{51}Cr release assay using E.G7-OVA cells (OVA-expressing cells), and its parental cell line, EL4 cells (OVA-non-expressing cells), was examined. We found that the CTL activity induced by i.p. administration of the Man-lipoplex was higher than that induced by i.m. or i.d. administration of the Man-lipoplex (Figure 3a).

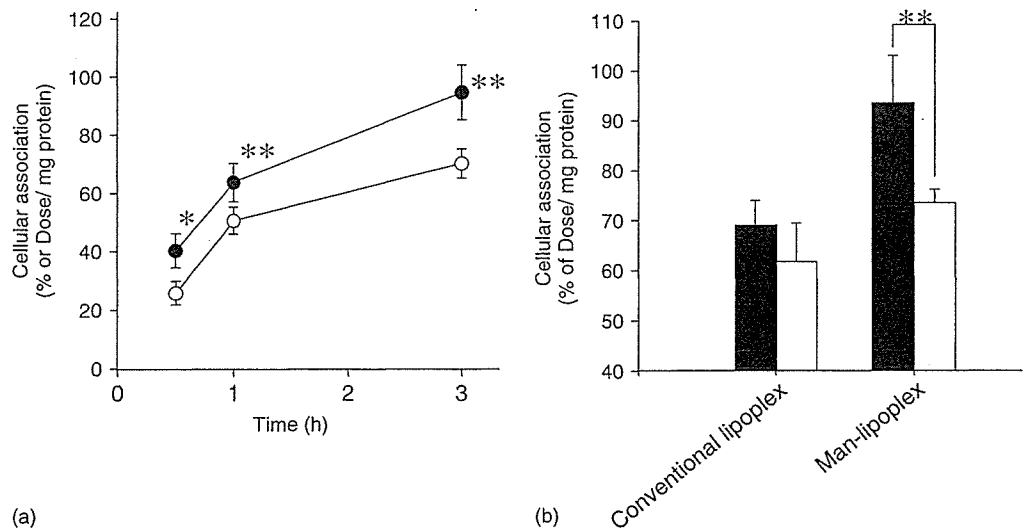

Figure 1. Cellular association of the Man-lipoplex in DC2.4 cells. (a) Cellular association time-course of ^{32}P-labeled Man-lipoplex (●) and lipoplex (○) in DC2.4 cells at 37 °C. pCMV-OVA (0.5 μg/ml) was complexed with cationic liposomes at a charge ratio (−/+) of 1.0 : 1.6. Each value represents the mean ± standard deviation (S.D.) ($n = 3$). (b) Cellular association of ^{32}P-labeled lipoplex or Man-lipoplex in the absence (■) or presence (□) of 0.125 mg/ml mannan in the culture medium. Each value represents the mean + S.D. ($n = 4$). Statistical analysis was performed by Student's *t*-test (*$P < 0.05$, **$P < 0.01$)

J Gene Med 2006; 8: 824–834.
DOI: 10.1002/jgm

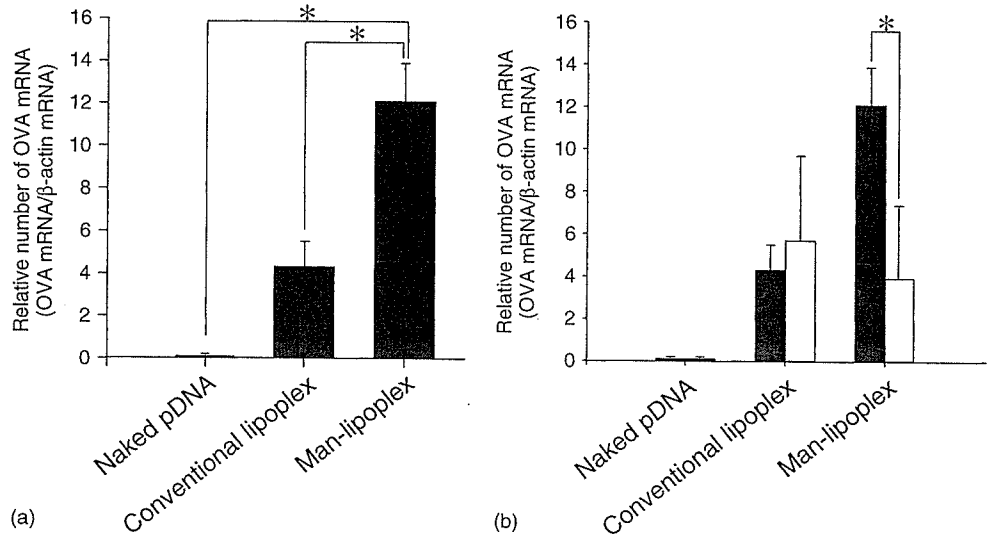

Figure 2. Transfection activity of the Man-lipoplex in DC2.4 cells. (a) Transfection activity of naked pCMV-OVA or lipoplexes in cultured DC2.4 cells. The concentration of pDNA was fixed at 0.5 μg/ml in all experiments. Each value represents the mean + S.D. (n = 3). (b) Transfection activity of naked pCMV-OVA or lipoplexes in the absence (■) or presence (□) of 0.125 mg/ml mannan. The concentration of pCMV-OVA was fixed at 0.5 μg/ml in all experiments. Each value represents the mean + S.D. values (n = 4). Statistical analysis was performed by analysis of variance (*$P < 0.05$)

Furthermore, increasing the amount of pCMV-OVA of the Man-lipoplex markedly enhanced the CTL response induced by i.p. administration (Figure 3b). Furthermore, the CTL activity of the Man-lipoplex following i.p. administration was significantly higher than that induced by i.m. administration of naked pCMV-OVA (Figure 3c).

Effect of lipoplex mannosylation on CTL response

As shown in Figure 4a, the Man-lipoplex induced a much higher CTL response than the conventional lipoplex. However, the Gal-lipoplex induced a much lower CTL response than the Man-lipoplex (Figure 4b), suggesting that the Man-lipoplex induces a strong CTL response via a mannose receptor-mediated mechanism.

Gene expression characteristics of Man-lipoplex on CD11c$^+$ cells in the spleen and peritoneal cavity after i.p. administration

To clarify the transfection activity of the Man-lipoplex with regard to DCs after i.p. administration, the OVA mRNA in the CD11c$^+$ cells in the spleen and peritoneal cavity was determined 6 h after i.p. administration of naked pCMV-OVA (100 μg) or Man-lipoplex and conventional lipoplex using quantitative RT-PCR. The relative copy number of OVA mRNA in the Man-lipoplex injected group was the highest of all in both peritoneal CD11c$^+$ cells (Figure 5a) and splenic CD11c$^+$ cells (Figure 5b).

Anti-tumor responses of Man-lipoplex after immunization

To assess the protective anti-tumor effect, EL4 and E.G7-OVA cells were transplanted into pre-immunized mice. Pre-immunization with the Man-lipoplex prolonged the survival time after transplantation of E.G7-OVA cells compared with pDNA or conventional lipoplex (Figure 6a). However, all formulations failed to prolong the survival rate after transplantation of EL4 cells (Figure 6b).

Discussion

DNA vaccine represents an exciting novel approach in vaccine development. The vaccine construct is created by insertion of a DNA encoding the desired antigen into a pDNA. The extent to which the pDNA is able to transfect cells is dependent on the application route and delivery carrier used. The encoded protein is then expressed in the transfected cells *in vivo* and, consequently, an immune response is elicited to the expressed antigen. However, to date, there have been few reports on *in vivo* gene therapy based on targeted non-viral gene delivery. In our series of experiments, we have been developing APC-selective *in vivo* gene carrier systems for use in gene therapy [22–24,32]. In the present study, we describe the Man-lipoplex given i.p. as a novel approach to enhance therapeutic potency of DNA vaccine therapy *in vivo*.

Since some clinical trials have involved the local administration of naked pDNA [7–9], we evaluated the OVA-specific CTL response following the local administration of naked pDNA. As shown in Figure 3c,